

## **Supplementary File 1**

### **Supplementary Notes**

#### **Section 1: Data**

##### **1. Stable Isotope Ratio Analysis using Isotope Ratio Mass Spectrometry (IRMS)**

Samples were ground to a fine powder and extracted with polar and non-polar solvents (dichloromethane and methanol) in soxhlet apparatus. Lipids were separated from the solvent-extracted dry mass.  $\delta^2\text{H}$ ,  $\delta^{13}\text{C}$ ,  $\delta^{15}\text{N}$ ,  $\delta^{18}\text{O}$  and  $\delta^{34}\text{S}$  were determined in the sample using Agroisolab standard method AIL-1.1c (2015-02).

Delta notation is used to represent the relative abundance of the heavy isotope in parts per thousand with respect to the zero-point reference standard for each stable isotope ratio using the formula:  $\delta = \frac{IR_{\text{sample}} - IR_{\text{standard}}}{IR_{\text{standard}}} \times 1000$ .

For the oxygen stable isotope ratio ( $\delta^{18}\text{O}$ ), the comparison is made against the Vienna Standard Mean Ocean Water (VSMOW) zero-point standard.  $\delta^2\text{H}$  is also reported relative to VSMOW,  $\delta^{13}\text{C}$  is reported relative to Vienna Pee Dee Belemnite (VPDB),  $\delta^{15}\text{N}$  is reported relative to Air, and  $\delta^{34}\text{S}$  is reported relative to Vienna Canyon Diablo Troilite (VCDT). The unit used for delta notation in SIRA is per mille (‰).

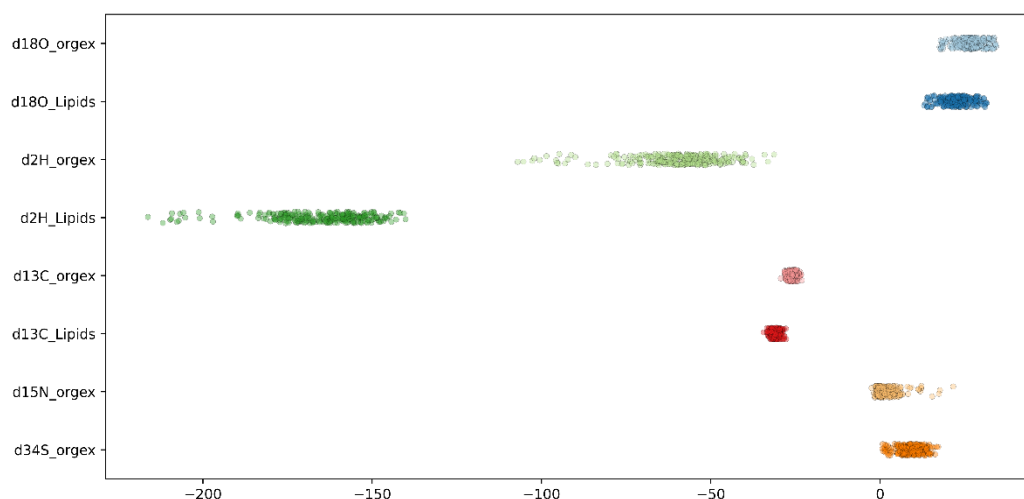


**Figure S1.** Scatterplot results of Stable Isotope Ratio Analysis (SIRA) for 267 soybean samples from South America. Results for Oxygen ( $\delta^{18}\text{O}$ ), Hydrogen ( $\delta^2\text{H}$ ), and Carbon ( $\delta^{13}\text{C}$ ) were measured from the lipid phase of the sample material (marked “Lipids” in the isotope ratio name) and from the non-lipid phase (marked “orgex”, for organic extraction). Nitrogen ( $\delta^{15}\text{N}$ ) and Sulphur ( $\delta^{34}\text{S}$ ) were measured in the non-lipid phase only. Quantities are isotope ratios (IR) relative to a commonly accepted standard (Oxygen – VSMOW; Hydrogen – VSMOW; Carbon – VPDB; Nitrogen – relative to air; Sulphur- VCDT).

## 2. Trace Element Analysis (ICP-MS)

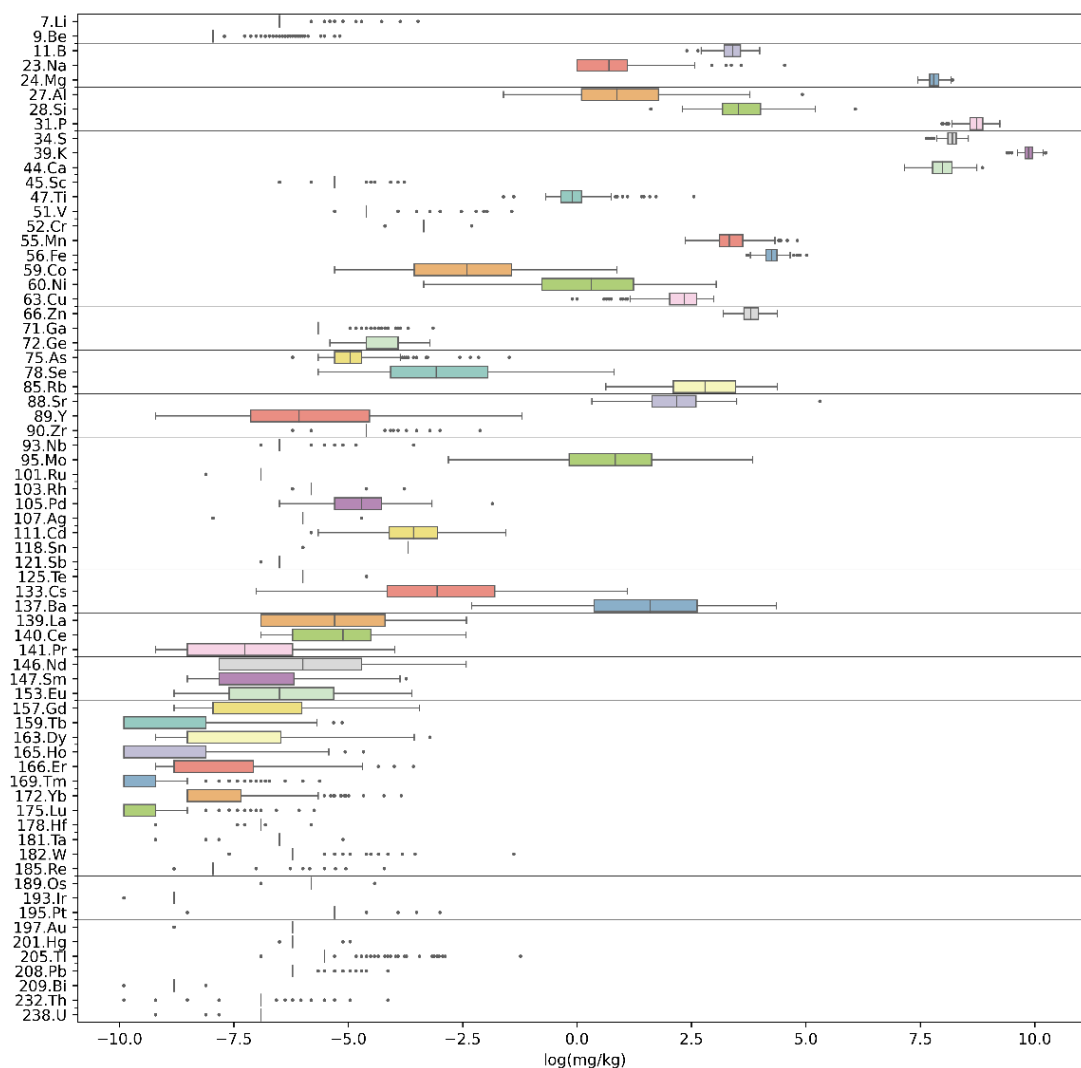


**Figure S2.** Boxplots summarise the detected levels (log-transformed) of 69 Elements in 267 soybean samples used in this study. The boxes represent the 2<sup>nd</sup> and 3<sup>rd</sup> quartiles of each distribution, whiskers denote the 1<sup>st</sup> and 4<sup>th</sup> quartiles, and dots indicate outliers, defined as exceeding 1.5 times the inter-quartile range. Colour added for visualization.

### 3. Data distribution in context

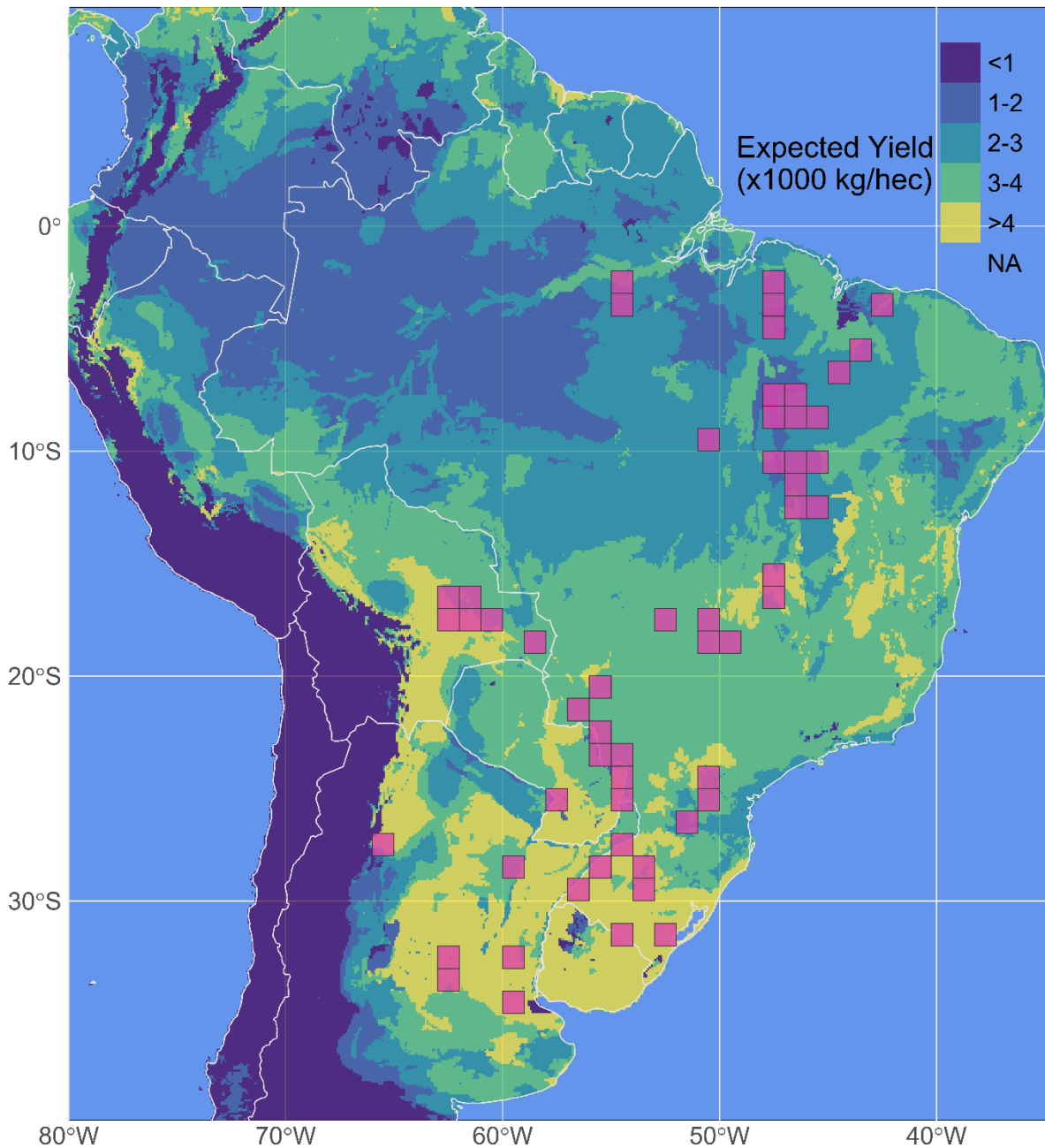


**Figure S3.** Map of the study area showing the harvest locations of 267 soybean samples used in this study. Pink 1° x 1° grid cells represent one or more sampling locations. These grid cells are used to anonymise collection locations and protect farmer/donor identity; modelling and spatial prediction were carried out on 0.133° x 0.133° grid cells. Soy suitability map based on global agro-ecological zones (FAO and IIASA, 2021). The prior we used for the Gaussian Process models only includes pixels where expected soybean yields exceed 2000 kg/hectare. Among those pixels, probability is distributed evenly (flat prior).

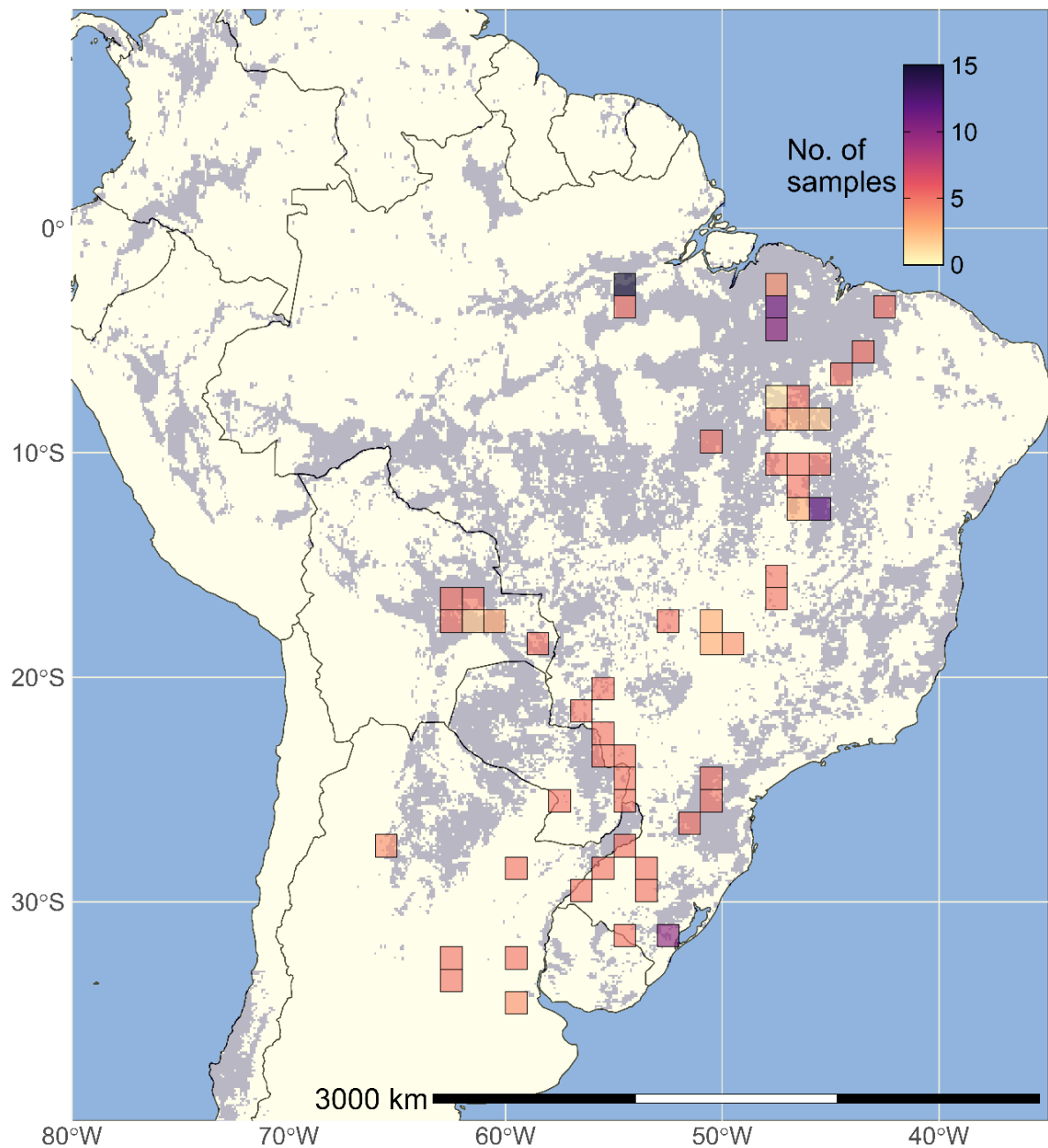


**Figure S4.** Map of the study area showing the harvest locations of 267 soybean samples used in this study. The colour of each 1° x 1° pixel represents the number of samples collected within its boundaries. The 1° x 1° grid cells are used in this figure to anonymise collection locations and protect farmer/donor identity; modelling and spatial prediction were carried out on 0.133° x 0.133° grid cells. Grey background marks forest cover loss between 2000-2023 (Source: Hansen/UMD/Google/USGS/NASA; Hansen et al., 2013; accessed on 28/01/2025). For a comprehensive overlay of deforestation and soybean farming please see this map from Global Forest Watch: <https://gfr.wri.org/forest-extent-indicators/deforestation-agriculture#how-much-forest-has-been-replaced-by-soy> (Goldman and Weisse, 2024).

## **Supplementary Methods**

### **Section 2: Quasi-classification on data subsets**

To test how a more balanced dataset might affect the predictive performance of the Gaussian Process (GP) model, we created two subsets of the data. For the first subset we omitted all data points to the north of latitude 15°S ( $n_{\text{north}}=110$ , 41% of total data; all from Brazil), then we re-fitted GP models for SIR, TE, or SIR + TE data, and quasi-classified the resulting coordinates to enable model performance comparison. We repeated this exercise for the second subset, where we omitted all data points between latitudes 15°S and 32°S, and east of longitude 57°W ( $n_{\text{centre}}=99$ , 37% of the data; 94 samples from Brazil and 5 from Argentina). Fitting the GP model to the smaller datasets also provides an indication to the effect of data scarcity on prediction accuracy.

Our model is a proof of concept, showing promising prediction accuracy, but also considerable error in some cases. Repeating the analysis pipeline after omitting the “north” or “centre” subsets expectedly increased classification error, reflecting the loss of information due to data omission. However, the GP model mapped some predictions into areas of omission that are adjacent to data points (Supp Fig. S5, S6, S7). Although this is evidence of prediction inaccuracy, it also demonstrates the ability of the GP model to account for regions not directly represented in the training data. We expect the accuracy of origin estimates to improve with the addition of reference samples from unsampled regions.

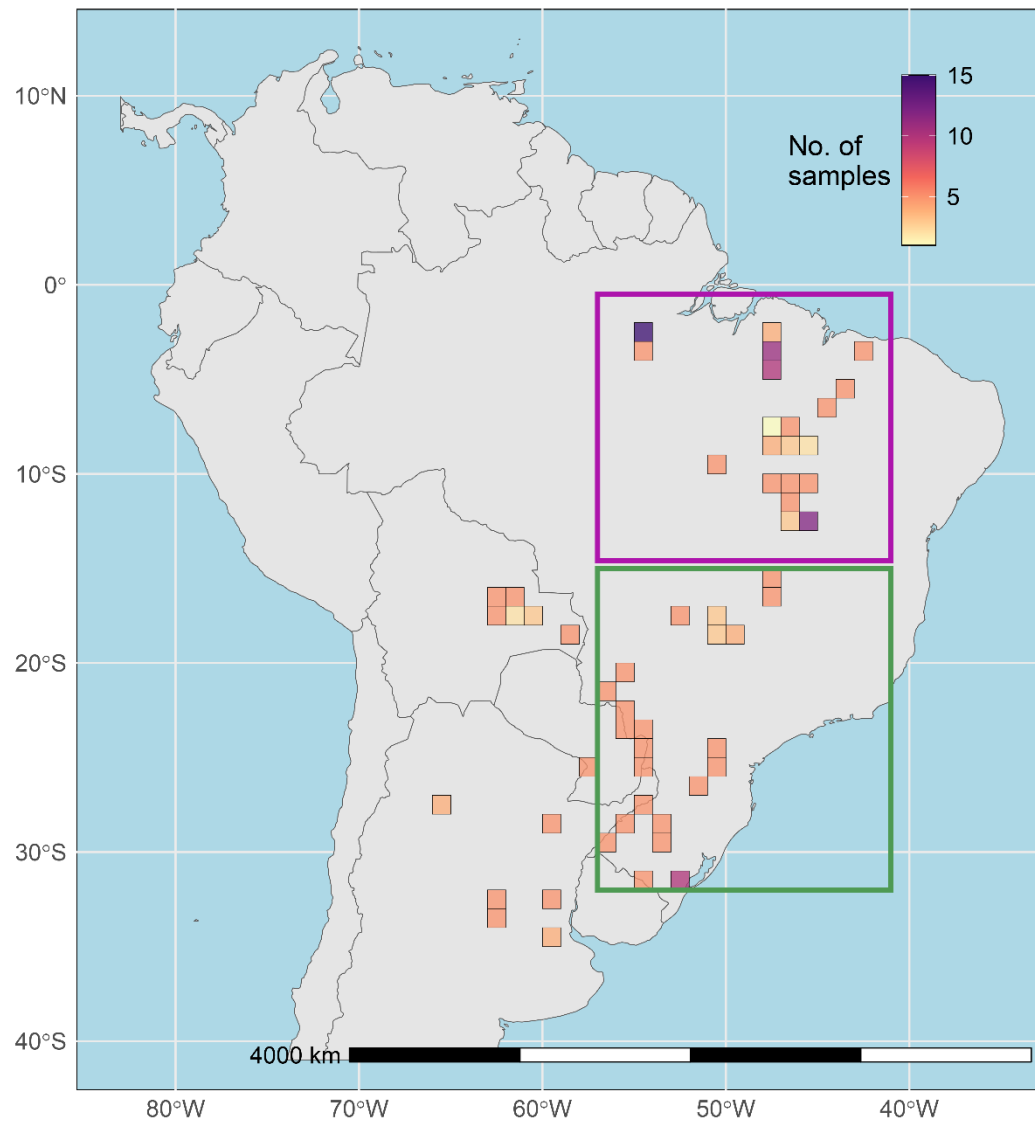


**Figure S5.** Pixel map of data distribution showing the extent of the data omission regions for quasi-classification experiments on data subsets. Pixel colour corresponds to number of samples. Purple rectangle (“north”) includes all samples north of 15°S ( $n_{\text{north}} = 110$ ); green rectangle (“centre”) includes samples between 15°S, 32°S, 57°W and 41°W ( $n_{\text{centre}} = 99$ ).

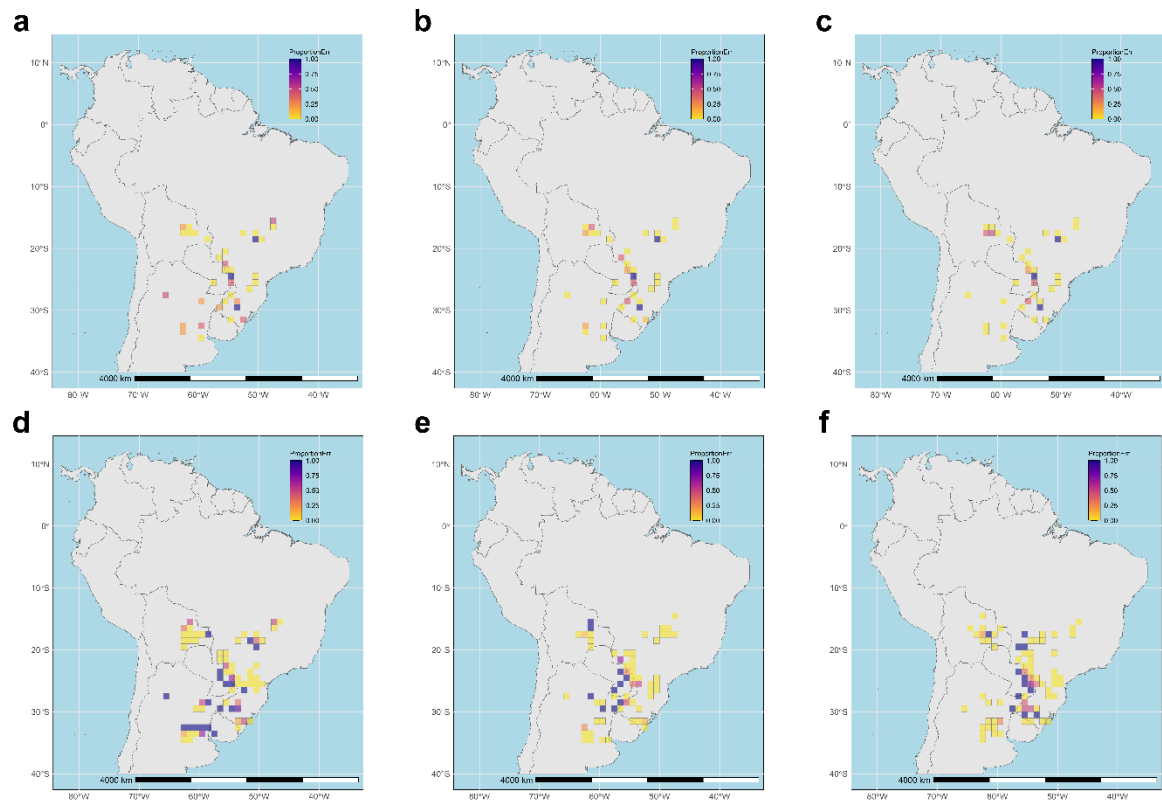


**Figure S6.** Quasi-classification of origin determination results from (a, d) the SIR, (b, e) TE, and (c, f) SIR + TE models, fit to the subset of the data that was harvested south of latitude 15°S. Coordinates were converted into the respective country to assess prediction correctness, and binned into pixels for visualisation. Panels a-c show proportion of prediction error by pixel of origin, panels d-f show proportion of prediction error by pixel of prediction.

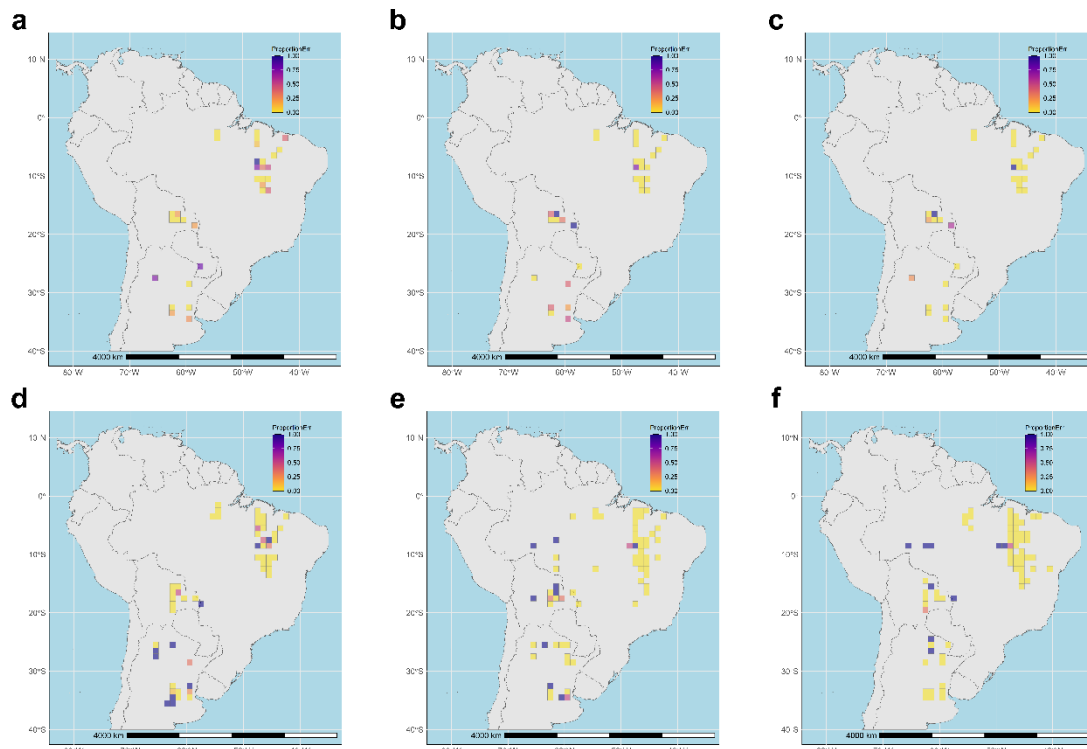


**Figure S7.** Quasi-classification of origin determination results from (a, d) the SIR, (b, e) TE, and (c, f) SIR + TE models, fit to the subset of the data harvested outside the region defined by latitudes 15°S and 32°S, and longitudes 57°W and 41°W. Coordinate were converted into the respective country and binned into pixels for visualisation. Panels a-c show proportion of prediction error by pixel of origin, panels d-f show proportion of prediction error by pixel of prediction.

### Section 3: Extended models

We Constructed extended models with climate and soil variables as predictors for inferring isotopic and elemental spatial distributions used as input for the origin determination model. Due to computational limitations we used a simplified version of the origin determination model, with 3 stable isotopes and 8 elemental predictors. For each of these 11 predictors we designed an independent GP model with up to 3 atmospheric or soil variables that are hypothesized to be driving its spatial distribution, based on previous studies on trees and other plants. For example, the oceans are the natural reservoir of heavy Hydrogen and Oxygen isotopes, so that the ratio of these isotopes in rainwater decreases with elevation and distance from the coast (Bowen, 2010; Pederzani & Britton, 2019; West et al., 2010). Temperature affects relative humidity as well as the plant's water uptake, leading to a complex mathematical relationship between temperature, heavy isotope availability in environmental water, and uptake (Bertoldi et al., 2016; Boeschoten et al., 2022; Hevia et al., 2018; Leavitt, 2010; Pederzani & Britton, 2019; Siegwolf et al., 2022; van der Sleen et al., 2017; Vargas et al., 2022; Wang et al., 2020; West et al., 2010, 2010; Zhao et al., 2024).



The environmental predictors linked to each isotope ratio or element are summarised in Table S1. We used climate data from CRU v4.07 (Harris et al., 2020), and soil data from SoilGrids2.0 (Poggio et al., 2021). The variables we used may not be the optimal environmental predictors for the compositional variables considered, but detailed literature for soybean is lacking. The spatial distribution of each SIR or TE was then inferred using a GP regression model taking the SIR/TE and additional environmental variables as predictors.

We compared the predictive performance of this extended model to the performance of the simpler models: Sir-only, TE-only, SIR+TE, and SIR+TE with climate data for SIR. Although more complex, the extended model demonstrated lower prediction precision and accuracy than the SIR+TE model and the TE-only model (Figs. S8, S9).

**Table S1.** Environmental predictors used in the extended GP model. Atmospheric variables are maximum-, minimum- and mean ambient temperature for the years 2021 and 2022. Soil variables are cation exchange capacity of the soil (cec), soil pH (phh2o), and bulk density of the fine earth fraction (bdod), at 5-15 cm below the surface.

Compositional variable	Environmental predictor/s
d18O_orgex	mean annual precipitation; maximum temperature
d2H_Lipids	mean annual precipitation; minimum temperature
d13C_orgex	mean annual precipitation; mean annual temperature
24.Mg	cec_5-15cm_mean; phh2o_5-15cm_mean
27.Al	cec_5-15cm_mean; phh2o_5-15cm_mean
28.Si	cec_5-15cm_mean; phh2o_5-15cm_mean
59.Co	cec_5-15cm_mean
60.Ni	bdod_5-15cm_mean; phh2o_5-15cm_mean
78.Se	cec_5-15cm_mean; phh2o_5-15cm_mean
88.Sr	bdod_5-15cm_mean; cec_5-15cm_mean; phh2o_5-15cm_mean
95.Mo	bdod_5-15cm_mean

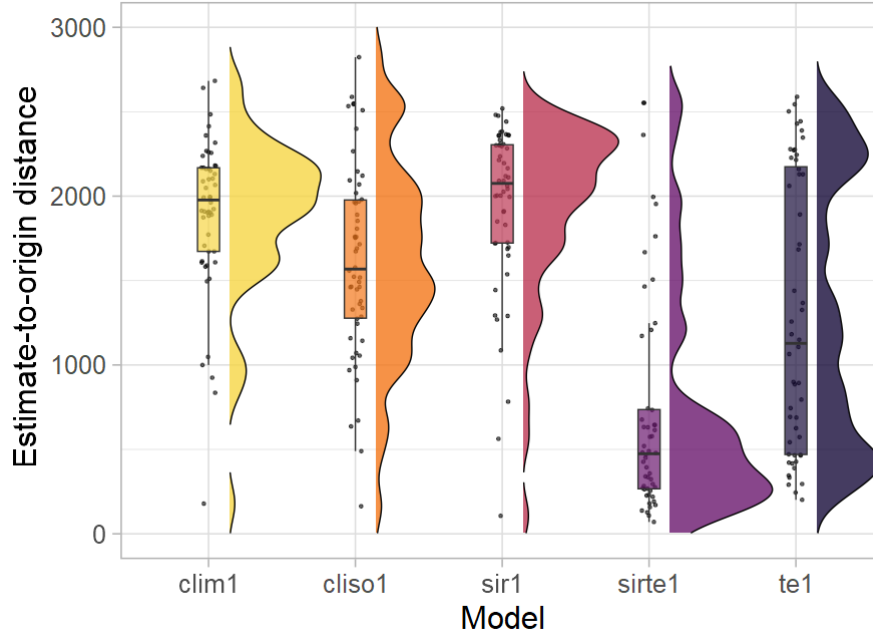


**Figure S8.** Prediction error by data type: clim– SIR and climate data; cliso– SIR, TE, climate, and soil data; sir– only SIR data; sirte– SIR and TE data; te– only TE data. Boxplots show quartiles, median values, and outliers ( $>2 \times \text{IQR}$ ) of the prediction error index. Due to computational limitations the models here are based on a smaller set of SIR and TE than the models presented in the main text.

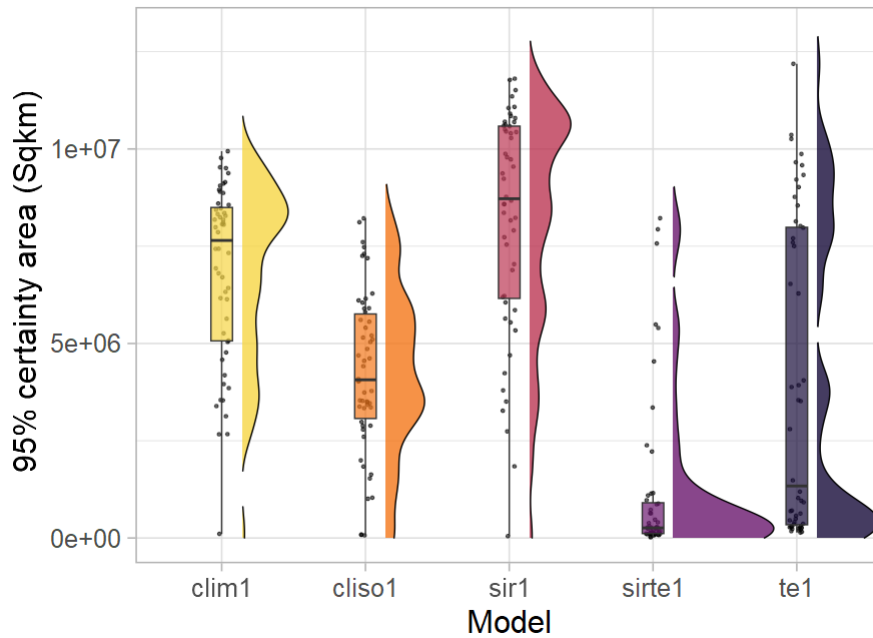


**Figure S9.** Prediction precision (95% Credible Region) index by data type: clim– SIR and climate data; cliso– SIR, TE, climate, and soil data; sir– only SIR data; sirte– SIR and TE data; te– only TE data. Boxplots show quartiles, median values, and outliers ( $>2 \times \text{IQR}$ ) of the 95% credible region. Due to computational limitations the models here consider a smaller set of SIR and TE than the models presented in the main text.

## **Supplementary Discussion**

### **Section 4: Climatic and environmental predictors**

We found that the most important isotope ratio for both latitude- and longitude prediction is  $\delta^2\text{H}$  from lipids, and the most important elements are nickel ( $^{60}\text{Ni}$ ), barium ( $^{137}\text{Ba}$ ), and cobalt ( $^{59}\text{Co}$ ). Terrain conditions such as elevation, slope, and distance to the coast are known to drive isotopic distributions, particularly Hydrogen and Oxygen isotopes (Siegwolf et al., 2022; West et al., 2010, 2010). Due to the lack of improvement in prediction metrics in the extended models, we decided against further extending the models with slope and elevation data (for distance to coast data, one has to first identify the relevant coast, based on weather patterns, seasonality, terrain etc.). However, the soy suitability data we used already integrates over the effects of variables relevant to soybean growth, which greatly simplified our models and enabled deeper examination of model parameter space.

The hydrogen isotopic ratio in terrestrial plants is governed by  $^2\text{H}$  availability in precipitation and atmospheric water, and varies with environmental factors such as temperature, elevation, latitude, distance from the coast, and others (Kagawa, 2022; Siegwolf et al., 2022; West et al., 2010). As  $\delta^2\text{H}$  mainly varies with abiotic processes, it is relatively predictable, making it a dependable spatial indicator. Ni and Co are essential for nitrogen fixation and metabolism, vital for commercial soybean production (Abreu-Junior et al., 2023; Eskew et al., 1983). Soybeans require soil Ni concentration within a narrow range, with substantial yield reductions outside of that range (Lavres et al., 2016; Sirhindi et al., 2016). Although this guarantees measurable levels of Ni in commercial soybeans (and consequently its utility as a spatial indicator), in the current dataset Ni levels span six orders of magnitude, indicating that Ni content in the soybeans is not determined solely by its concentration in the soil. In Brazil, Ni is ubiquitous in soy growing regions, but the factors that modify its uptake, primarily soil pH and cation exchange capacity (Macedo et al., 2016, 2020), vary with natural soil properties and farming practices and can be spatially informative. Ba is ubiquitous in the environment and occurs in legumes in high concentrations as its uptake follows Ca uptake (Cappuyns, 2018; Myrvang et al., 2016), but excess Ba inhibits photosynthesis in soybean (Suwa et al., 2008). Liming, which lowers the Ba:Ca ratio in the plant tissue, is commonly practiced in soybean farms, particularly on leached and acidic tropical soils, to control soil pH and provide the nutrients needed for efficient nitrogen fixation (Fageria & Stone, 2008; Macedo et al., 2020). However, liming must be limited to avoid inhibition of K and Mg uptake by Ca (Myrvang et al., 2016), which stabilises soybean Ba concentrations at detectable levels. Liming does not remediate Ni, Co, or Mo deficiency, which are supplied to soybeans separately

(Abreu-Junior et al., 2023; Macedo et al., 2016). Ni and Co commonly co-occur, their mineralisation, distribution, and mobility a result of soil geochemistry and may be affected by farming practices more than by climate and hydrology, yet they are useful spatial indicators. We hypothesise that although soil concentrations of these elements are largely independent of environmental variables such as temperature or humidity, their uptake to the plant is environmentally driven, which generated the spatial signal picked up by the GP model.

The GP model used here relies solely on a sample's chemical composition to infer harvest origin. Including environmental factors, such as temperature, precipitation, altitude, and soil type, that govern elemental and isotopic distribution across landscapes, could further refine estimates by accounting for physiological processes like hydraulics, carbon sequestration, and nitrogen fixation (DeNiro & Epstein, 1977; Kagawa, 2022; Schmiede et al., 2023; Zhao et al., 2024). This may reduce prediction uncertainty at locations away from data points and improve accuracy without needing costly additional samples.

However, the relationships between plant chemical composition and environmental factors are complex and only partly understood (Siegwolf et al., 2022; Vargas et al., 2022; Werner et al., 2012; Wigganhauser et al., 2022; Yakir & Sternberg, 2000), impeding the inclusion of these processes into the GP framework. For example, the ratios among element pairs may be more useful for traceability than their absolute quantities (Hevia et al., 2018; Kuang et al., 2008). Our extended models, not based on soy-specific literature (which is lacking) correlated isotope ratios with climate and element abundance with soil properties, but were highly computationally demanding and did not improve prediction accuracy (data not shown). Using additional data (such as genetic markers) may help refine origin estimates.

Long-lived species' chemical composition measurements for origin identification are often multi-year averages (Hagemeyer et al., 1992; Mortier et al., 2024; Scharnweber et al., 2016; Siegwolf et al., 2022; Truszkowski et al., 2025), whereas annual species reflect single-year or season conditions, which may vary considerably year-on-year. Whereas trees exhibit within-individual variation in elemental content (Hevia et al., 2018), in annual species this variation reflects both environmental conditions and individual differences, without a multi-year reference to help tease them apart. Crop species, particularly modern varieties grown outside their domestication centres, have reduced genetic diversity which may reduce variation in individual responses to environmental conditions. Our data maximises spatial coverage without resampling. Future data accumulation, including environmental data from the year of sample collection, may enable modelling temporal variation in soybean composition, accounting for environmental variability.

## **Supplementary References**

- Abreu-Junior, C. H., Gruberger, G. A. C., Cardoso, P. H. S., Gonçalves, P. W. B., Nogueira, T. A. R., Capra, G. F., & Jani, A. D. (2023). Soybean Seed Enrichment with Cobalt and Molybdenum as an Alternative to Conventional Seed Treatment. *Plants*, 12(5), 1164. <https://doi.org/10.3390/plants12051164>
- Bertoldi, D., Barbero, A., Camin, F., Caligiani, A., & Larcher, R. (2016). Multielemental fingerprinting and geographic traceability of Theobroma cacao beans and cocoa products. *Food Control*, 65, 46–53. <https://doi.org/10.1016/j.foodcont.2016.01.013>
- Boeschoten, L. E., Sass-Klaassen, U., Vlam, M., Comans, R. N. J., Koopmans, G. F., Meyer-Sand, B. R. V., Tassiamba, S. N., Tchamba, M. T., Zanguim, H. T., Zemtsa, P. T., & Zuidema, P. A. (2022). Clay and soil organic matter drive wood multi-elemental composition of a tropical tree species: Implications for timber tracing. *Science of The Total Environment*, 849, 157877. <https://doi.org/10.1016/j.scitotenv.2022.157877>
- Bowen, G. J. (2010). Isoscapes: Spatial Pattern in Isotopic Biogeochemistry. In *Annual Review of Earth and Planetary Sciences* (Vol. 38, Issue Volume 38, 2010, pp. 161–187). Annual Reviews. <https://doi.org/10.1146/annurev-earth-040809-152429>
- Cappuyns, V. (2018). Barium (Ba) leaching from soils and certified reference materials. *Applied Geochemistry*, 88, 68–84. <https://doi.org/10.1016/j.apgeochem.2017.05.002>
- DeNiro, M. J., & Epstein, S. (1977). Mechanism of Carbon Isotope Fractionation Associated with Lipid Synthesis. *Science*, 197(4300), 261–263. <https://doi.org/10.1126/science.327543>
- Eskew, D. L., Welch, R. M., & Cary, E. E. (1983). Nickel: An Essential Micronutrient for Legumes and Possibly All Higher Plants. *Science*, 222(4624), 621–623. <https://doi.org/10.1126/science.222.4624.621>
- Fageria, N. K., & Stone, L. F. (2008). Micronutrient Deficiency Problems in South America. In B. J. Alloway (Ed.), *Micronutrient Deficiencies in Global Crop Production* (pp. 245–266). Springer Netherlands. [https://doi.org/10.1007/978-1-4020-6860-7\\_10](https://doi.org/10.1007/978-1-4020-6860-7_10)
- FAO and IIASA. (2021). *Global Agro-Ecological Zones (GAEZ v4)* [Dataset]. FAO and IIASA. <https://gaez.fao.org/pages/data-viewer-theme-4>
- Goldman, E., & Weisse, M. (2024). *How much forest has been replaced by soy?* Global Forest Watch. <https://gfr.wri.org/forest-extent-indicators/deforestation-agriculture#how-much-forest-has-been-replaced-by-soy>

- Hagemeyer, J., Lülfsmann, A., Perk, M., & Breckle, S.-W. (1992). Are There Seasonal Variations of Trace Element Concentrations (Cd, Pb, Zn) in Wood of Fagus Trees in Germany? *Vegetatio*, 101(1), 55–63.
- Hansen, M. C., Potapov, P. V., Moore, R., Hancher, M., Turubanova, S. A., Tyukavina, A., Thau, D., Stehman, S. V., Goetz, S. J., Loveland, T. R., Kommareddy, A., Egorov, A., Chini, L., Justice, C. O., & Townshend, J. R. G. (2013). High-Resolution Global Maps of 21st-Century Forest Cover Change. *Science*, 342(6160), 850–853.  
<https://doi.org/10.1126/science.1244693>
- Harris, I., Osborn, T. J., Jones, P., & Lister, D. (2020). Version 4 of the CRU TS monthly high-resolution gridded multivariate climate dataset. *Scientific Data*, 7(1), 109.  
<https://doi.org/10.1038/s41597-020-0453-3>
- Hevia, A., Sánchez-Salguero, R., Camarero, J. J., Buras, A., Sangüesa-Barreda, G., Galván, J. D., & Gutiérrez, E. (2018). Towards a better understanding of long-term wood-chemistry variations in old-growth forests: A case study on ancient Pinus uncinata trees from the Pyrenees. *Science of The Total Environment*, 625, 220–232.  
<https://doi.org/10.1016/j.scitotenv.2017.12.229>
- Kagawa, A. (2022). Foliar water uptake as a source of hydrogen and oxygen in plant biomass. *Tree Physiology*, 42(11), 2153–2173. <https://doi.org/10.1093/treephys/tpac055>
- Kuang, Y. W., Wen, D. Z., Zhou, G. Y., Chu, G. W., Sun, F. F., & Li, J. (2008). Reconstruction of soil pH by dendrochemistry of Masson pine at two forested sites in the Pearl River Delta, South China. *Annals of Forest Science*, 65(8), 804–804.  
<https://doi.org/10.1051/forest:2008070>
- Lavres, J., Castro Franco, G., & De Sousa Câmara, G. M. (2016). Soybean Seed Treatment with Nickel Improves Biological Nitrogen Fixation and Urease Activity. *Frontiers in Environmental Science*, 4. <https://doi.org/10.3389/fenvs.2016.00037>
- Leavitt, S. W. (2010). Tree-ring C–H–O isotope variability and sampling. *Science of The Total Environment*, 408(22), 5244–5253. <https://doi.org/10.1016/j.scitotenv.2010.07.057>
- Macedo, F. G., Bresolin, J. D., Santos, E. F., Furlan, F., Lopes Da Silva, W. T., Polacco, J. C., & Lavres, J. (2016). Nickel Availability in Soil as Influenced by Liming and Its Role in Soybean Nitrogen Metabolism. *Frontiers in Plant Science*, 7.  
<https://doi.org/10.3389/fpls.2016.01358>
- Macedo, F. G., Santos, E. F., & Lavres, J. (2020). Agricultural crop influences availability of nickel in the rhizosphere; a study on base cation saturations, Ni dosages and crop succession. *Rhizosphere*, 13, 100182. <https://doi.org/10.1016/j.rhisph.2019.100182>

- Mortier, T., Truszkowski, J., Norman, M., Boner, M., Buliga, B., Chater, C., Jennings, H., Saunders, J., Sibley, R., Antonelli, A., Waegeman, W., & Deklerck, V. (2024). A framework for tracing timber following the Ukraine invasion. *Nature Plants*. <https://doi.org/10.1038/s41477-024-01648-5>
- Myrvang, M. B., Bleken, M. A., Krogstad, T., Heim, M., & Gjengedal, E. (2016). Can liming reduce barium uptake by agricultural plants grown on sandy soil? *Journal of Plant Nutrition and Soil Science*, 179(4), 557–565. <https://doi.org/10.1002/jpln.201600104>
- Pederzani, S., & Britton, K. (2019). Oxygen isotopes in bioarchaeology: Principles and applications, challenges and opportunities. *Earth-Science Reviews*, 188, 77–107. <https://doi.org/10.1016/j.earscirev.2018.11.005>
- Poggio, L., de Sousa, L. M., Batjes, N. H., Heuvelink, G. B. M., Kempen, B., Ribeiro, E., & Rossiter, D. (2021). SoilGrids 2.0: Producing soil information for the globe with quantified spatial uncertainty. *SOIL*, 7(1), 217–240. <https://doi.org/10.5194/soil-7-217-2021>
- Scharnweber, T., Hevia, A., Buras, A., Van Der Maaten, E., & Wilmking, M. (2016). Common trends in elements? Within- and between-tree variations of wood-chemistry measured by X-ray fluorescence — A dendrochemical study. *Science of The Total Environment*, 566–567, 1245–1253. <https://doi.org/10.1016/j.scitotenv.2016.05.182>
- Schmiege, S. C., Heskel, M., Fan, Y., & Way, D. A. (2023). It's only natural: Plant respiration in unmanaged systems. *Plant Physiology*, 192(2), 710–727. <https://doi.org/10.1093/plphys/kiad167>
- Siegwolf, R. T. W., Brooks, J. R., Roden, J., & Saurer, M. (Eds.). (2022). *Stable Isotopes in Tree Rings: Inferring Physiological, Climatic and Environmental Responses* (Vol. 8). Springer International Publishing. <https://doi.org/10.1007/978-3-030-92698-4>
- Sirhindi, G., Mir, M. A., Abd-Allah, E. F., Ahmad, P., & Guzel, S. (2016). Jasmonic Acid Modulates the Physio-Biochemical Attributes, Antioxidant Enzyme Activity, and Gene Expression in Glycine max under Nickel Toxicity. *Frontiers in Plant Science*, 7. <https://doi.org/10.3389/fpls.2016.00591>
- Suwa, R., Jayachandran, K., Nguyen, N. T., Boulenouar, A., Fujita, K., & Saneoka, H. (2008). Barium Toxicity Effects in Soybean Plants. *Archives of Environmental Contamination and Toxicology*, 55(3), 397–403. <https://doi.org/10.1007/s00244-008-9132-7>
- Truszkowski, J., Maor, R., Yousuf, R. B., Biswas, S., Chater, C., Gasson, P., McQueen, S., Norman, M., Saunders, J., Simeone, J., Ramakrishnan, N., Antonelli, A., & Deklerck, V. (2025). A probabilistic approach to estimating timber harvest location. *Ecological Applications*, 35(1), e3077. <https://doi.org/10.1002/eap.3077>

- van der Sleen, P., Zuidema, P. A., & Pons, T. L. (2017). Stable isotopes in tropical tree rings: Theory, methods and applications. *Functional Ecology*, 31(9), 1674–1689.  
<https://doi.org/10.1111/1365-2435.12889>
- Vargas, D., Pucha-Cofrep, D., Serrano-Vincenti, S., Burneo, A., Carlosama, L., Herrera, M., Cerna, M., Molnár, M., Jull, A. J. T., Temovski, M., László, E., Futó, I., Horváth, A., & Palcsu, L. (2022). ITCZ precipitation and cloud cover excursions control *Cedrela nebulosa* tree-ring oxygen and carbon isotopes in the northwestern Amazon. *Global and Planetary Change*, 211, 103791. <https://doi.org/10.1016/j.gloplacha.2022.103791>
- Wang, Z., Erasmus, S. W., Dekker, P., Guo, B., Stoorvogel, J. J., & Ruth, S. M. van. (2020). Linking growing conditions to stable isotope ratios and elemental compositions of Costa Rican bananas (*Musa* spp.). *Food Research International*, 129, 108882.  
<https://doi.org/10.1016/j.foodres.2019.108882>
- Werner, C., Schnyder, H., Cuntz, M., Keitel, C., Zeeman, M. J., Dawson, T. E., Badeck, F.-W., Brugnoli, E., Ghashghaie, J., Grams, T. E. E., Kayler, Z. E., Lakatos, M., Lee, X., Máguas, C., Ogée, J., Rascher, K. G., Siegwolf, R. T. W., Unger, S., Welker, J., ... Gessler, A. (2012). Progress and challenges in using stable isotopes to trace plant carbon and water relations across scales. *Biogeosciences*, 9(8), 3083–3111. <https://doi.org/10.5194/bg-9-3083-2012>
- West, J. B., Bowen, G. J., Dawson, T. E., & Tu, K. P. (2010). *Isoscapes: Understanding movement, pattern, and process on Earth through isotope mapping*. Springer.
- Wiggenhauser, M., Moore, R. E. T., Wang, P., Bienert, G. P., Laursen, K. H., & Blotevogel, S. (2022). Stable Isotope Fractionation of Metals and Metalloids in Plants: A Review. *Frontiers in Plant Science*, 13, 840941. <https://doi.org/10.3389/fpls.2022.840941>
- Yakir, D., & Sternberg, L. D. S. L. (2000). The use of stable isotopes to study ecosystem gas exchange. *Oecologia*, 123(3), 297–311. <https://doi.org/10.1007/s004420051016>
- Zhao, L., Liu, X., Wang, N., Barbeta, A., Zhang, Y., Cernusak, L. A., & Wang, L. (2024). The determining factors of hydrogen isotope offsets between plants and their source waters. *New Phytologist*, 241(5), 2009–2024. <https://doi.org/10.1111/nph.19492>